Dipole-Field Sums, Lorentz Factors, and Dielectric Properties of Organic Molecular Films Modeled as Crystalline Arrays of Polarizable Points

*Davide Vanzo, Benjamin J. Topham, and Zoltán G. Soos**

The relative permittivity $\kappa = \varepsilon/\varepsilon_0$ of thin films used in organic electronic devices is directly related to the structure and the molecular polarizability α when intermolecular overlap is small. Monolayer and multilayer films are modeled as lattices of polarizable points with induced dipoles $\mu = \alpha F$ where the internal electric field F includes contributions from all induced dipoles. The polarization per unit volume is $P = n\mu$ for number density n. Dipole-field sums are evaluated directly for atomic and molecular crystals and films through stacking of infinite layers. Lorentz factors in uniformly polarized crystals of less than cubic symmetry resolve completely the conditional convergence of dipole-field sums in three dimensions. Thin films have equal P within layers but not at or near the surface. Surface effects are shown to increase with αn and sometimes to extend into films even though dipole fields are mainly due to adjacent layers. Simple and body-centered tetragonal lattices illustrate polarizing or depolarizing interactions between layers that mimic molecules or oligomers tilted at angle Φ from normal to the surface in films or SAMs. Uniform P in molecular films refers to unit cells rather than to atoms and there are multiple ways to partition anisotropic molecular α among polarizable points. An illustrative analytical model based on polarizable points and dipole fields of adjacent layers is applied to oligophenyl films and to conjugated molecules in acene films.

1. Introduction

Molecular thin films play a central role in organic electronic devices. Organic light emitting diodes, transistors or photovoltaic systems contain multiple films of nanometer thickness d. Films with designed electronic functions and controlled thickness are made possible by weak interactions between closed-shell molecules with small intermolecular overlap. Small d compensates for the limited mobility of charges, typically by hopping transport, in low dielectric insulators. The formation and characterization of organic thin films has been the focus of sustained research for decades. Theoretical modeling and understanding has likewise been extensive.

Dr. D. Vanzo, Prof. B. J. Topham,[+] Prof. Z. G. Soos
Department of Chemistry
Princeton University
Princeton, NJ 08544, USA
E-mail: soos@princeton.edu
[+]Present address: Department of Chemistry and Physics, Longwood University, Farmville, VA 23909, USA

DOI: 10.1002/adfm.201402405

Density functional theory (DFT) has been the method of choice for the study of the electronic structure of organic thin films, self-assembled monolayers (SAMs) or metal–organic interfaces. Dielectric properties are modeled by applying a constant electric field across a film or SAM whose structure is taken from experiment, calculated or simply assumed. DFT is best at intermediate lengths scales, longer than molecular but well short of macroscopic except in periodic systems. Before such calculations were feasible, molecular exciton theory was used to investigate the optical properties of organic molecular crystals, notably naphthalene and anthracene. Weak intermolecular interactions between closed-shell molecules are naturally treated as a perturbation. An applied electric field or Coulomb interactions between molecular ions may also be treated as perturbations, now with infinite range. A basic approximation is to neglect overlap between molecules even though overlap is mandatory for charge transport and hence for electronics applications. Zero overlap makes possible a general rather than film-by-film discussion of dielectric properties. In this work, we model films of nanometer thickness and macroscopic area using two methods that neglect intermolecular overlap.

In microelectrostatic (ME) theory,[1,2] molecules in organic crystals are represented by one or several polarizable points in order to model classical electrostatic interactions. Alternatively, intramolecular charge redistribution (CR) describes classical electrostatics between quantum molecules that do not overlap.[3] ME and CR are inherently multiscale, using the best available molecular and structural inputs from experiment or theory to investigate long-range interactions in a unified manner. Atomic or ionic solids have routinely been modeled as lattices, and lattices of polarizable points become continuous dielectrics on length scales longer than lattice constants.

We consider films of polarizable points and find the total field F due to an applied field E and induced dipoles $\mu = \alpha F$. For scalar polarizability α and cubic crystals, Lorentz showed that

$$F = fE = E/(1 - 4\pi\alpha n L) \quad (1)$$

where $n = N/V$ is the number density and $L = 1/3$ is the Lorentz factor. Induced dipoles increase E by the factor f. Total F with $L = 1/3$ also follows from the Clausius-Mossotti equation (CME) that relates[4,5] the relative permittivity $\kappa = \varepsilon/\varepsilon_0$ of a macroscopic gaseous or liquid sample to α

$$\frac{\kappa - 1}{\kappa + 2} = \frac{4\pi\alpha n}{3} \tag{2}$$

The factor 4π in Gaussian units is replaced by $1/\varepsilon_0$ in MKS units, where $\varepsilon_0 = 8.58 \times 10^{-12}$ F/m. Scalar α and equal F at all sites always lead to f in Equation 1 but L deviates from 1/3 in lower than cubic symmetry and depends on the direction of E. In such cases, f is no longer isotropic, $f < 1$ is possible in some direction and scalar α leads to anisotropic (tensor) κ. Significant enhancement f is possible although so far divergent f and spontaneous polarization have not been reported.

Following Allen,[6] we refer to the generalized CME whenever $F = fE$ but $L \neq 1/3$, and we also study molecular films with anisotropic α. We obtain Lorentz factors for films as a function of structure, thickness and αn. A rough estimate gives $\alpha n \approx 0.10$ for molecular volumes of 500 Å^3 and polarizability 50 Å^3; the CME with a typical $\kappa = 3$ for organic solids also yields $\alpha n \approx 0.10$.

Classical electrostatics describes the dielectric properties of continuous matter. Applications to nanocrystals or thin films must address discrete atoms or molecules in at least one dimension. It has been suggested that the CME holds down to one lattice constant.[7,8] Direct evaluation of Lorentz factors and dipole-field sums in films leads to a more nuanced estimate of 1–5 nm for the generalized CME. Textbook derivations[9,10] of the CME avoid dipole-field sums by considering cubic lattices in which the sums vanish by symmetry. Dipole-field sums converge conditionally in three-dimensional (3D) lattices and absolutely in 2D lattices such as a monolayer (ML). Mueller[11] long ago computed Lorentz factors that deviate from $L = 1/3$ in tetragonal lattices. As known since Maxwell, uniform polarization requires a sample whose surface is a general ellipsoid or a limiting case of a general ellipsoid. Colpa[12] has analyzed the physics of Lorentz factors and dipole-field sums in uniformly polarized or magnetized 3D samples. The evaluation of dipole-field sums is a longstanding topic,[11–14] first with analytical methods and then supplemented with computers. Direct evaluation of sums is now straightforward and used in this study.

The paper is organized as follows. In Section 2 we find Lorentz factors for uniformly polarized tetragonal lattices with isotropic α. Thick films with different surfaces and spherical crystals lead to identical L_c and L_a for E applied along the c and a crystallographic axes. We also compute 2D dipole-field sums in a ML and interlayer dipole fields in multilayers under the assumption of uniform polarization. In Section 3 we consider tetragonal films with uniform polarization within layers but not at or near the surface. Surface effects quantify deviations from the generalized CME. A simple analytical model gives the dependence of surface effects on αn and structure. In Section 4 we generalize to molecular crystals with anisotropic α and several molecules with dozens of atoms per unit cell. Uniform polarization now refers to unit cells and either spheres or layers yield the anisotropic $\kappa = \varepsilon/\varepsilon_0$ of crystals. Modeling organic thin films or SAMs as polarizable points is sketched in Section 5. The layer-by-layer calculation of dipole-field sums accounts naturally for the evolution of dielectric properties from ML to thick films. Section 6 briefly summarizes results for atomic and molecular films.

2. Dipole-Field Sums and Lorentz Factors

Equal local field F at all points corresponds to uniform polarization $P = n\mu = n\alpha F$ or, more generally, $\boldsymbol{P} = n\alpha \cdot \boldsymbol{F}$ for tensor α. Uniform P in a continuous dielectric requires a sample whose surface is a general ellipsoid or a limiting case of a general ellipsoid. We consider a lattice of N points $\{\boldsymbol{r}_s\}$ with tensor polarizability α_s. Quite generally, the electric field at a point taken as the origin is

$$\overrightarrow{F_0} = \overrightarrow{E_0} + \sum_m T_{0m} \cdot \alpha_m \cdot \overrightarrow{F_m} \tag{3}$$

The field $\boldsymbol{E}_0$ is due to fixed sources such as charges, dipoles, and so on. The second term is the contribution from induced dipoles $\boldsymbol{\mu}_m = \alpha_m \cdot \boldsymbol{F}_m$ with $m \neq 0$. The dipole-field tensor T_{nm} is a purely geometrical quantity, discussed later, that depends on $\{\boldsymbol{r}_s\}$. Systems of polarizable points, fixed sources and induced dipoles come up in many fields and Equation 3 is a physical statement about the total field at any site. For given fixed sources, a lattice of N points leads to a system of $3N$ linear equations for the components of $\boldsymbol{F}_p$. The electrostatic energy of the system is[1,2]

$$E_{\mathrm{el}}(\{n\}) = -\frac{1}{2}\sum_p \overrightarrow{E_{0p}} \cdot \alpha_p \cdot \overrightarrow{F_p} \tag{4}$$

The sum is over all lattice points p and $\boldsymbol{E}_{0p}$ is the field at p due to fixed sources; a lattice of neutral points has $\boldsymbol{E}_{0p} = 0$ for all p. The electrostatic (polarization) energy of a finite lattice with a positive ion at point r depends on the location of the charge. Equation 4 with atomic α accounts for core hole spectra of nanoclusters of noble gases.[15] The molecular α_p is partitioned among atoms in the ME approach[1,2] to E_{el}.

We will consider a uniform external field $\boldsymbol{E}_0 = \boldsymbol{E}$ and extended atomic or molecular lattices, starting with scalar α and atomic lattices in this Section. The solution of Equation 3 is disarmingly simple, at least formally, when $\boldsymbol{F}_m$ is the same at all points and the sample is an ellipsoid whose semi-major axes coincide with the principal axes of the dipole-field tensor Λ. Uniform E along a principal axis leads to collinear $\boldsymbol{F}$ and $\boldsymbol{E}$ with[12]

$$F = E/(1 - 4\pi n\alpha(D + \Lambda)) \tag{5}$$

Here $4\pi\Lambda = \Sigma_m T_{0m}$ is the dipole field at the origin, to be evaluated, and D is the depolarization factor. We note the similar forms of Equation 1,5. Textbooks[9,10] mention depolarization or demagnetization factors[16] but focus on cubic lattices with $\Lambda = 0$ by symmetry and $D = 1/3$. Colpa[12] discussed in detail the Lorentz tensor $L(\boldsymbol{r}) = D(\boldsymbol{r}) + \Lambda(\boldsymbol{r})$ at any point in terms of the depolarization and dipole-field tensors. The traces of L, D and Λ are 1, 1, and 0, respectively. Other works[13,14] address the conditional convergence of Λ, that is, the infinite sum over T_{0m} in Equation 3.

Bulk calculations typically invoke spherical samples. Mueller[11] reported Lorentz factors using the Ewald method for dipole-field sums in both real and reciprocal space. Purvis and Taylor[13] calculated Lorentz factors of orthorhombic and body-centered orthorhombic lattices using special functions and reciprocal space. However, direct summation in real space is straightforward with modern computational resources. For example, if a sphere of increasing radius R is embedded in the infinite lattice, $R = 10^3$ lattice constants return dipole-field sums in Equation 5 accurate to 5–6 significant figures, and larger R can readily be used.

We model the dielectric properties of films using tetragonal lattices with lattice constants a, a, c and E along or normal to the symmetry axis. The simple lattice has number density $n = 1/a^2c$. The body-centered lattice with the same n has larger lattice constants by $2^{1/3}$. Lorentz factors $L_c(c/a)$ or $L_a(c/a)$ refer to E along or normal to the c axis, with $L_c + 2L_a = 1$ for tetragonal symmetry. **Figure 1** shows $L_c(c/a)$ and unit cells of tetragonal lattices as a function of c/a. The strikingly different c/a dependence of simple and body-centered lattices is due to different interactions between adjacent planes along the c axis. Adjacent planes are eclipsed and polarizing in the simple lattice. They are displaced or staggered by $a/2$, $a/2$ in the body-centered lattice and depolarizing. The simple lattice has negative L_c and $f < 1$ for $c/a > 1.3988$, when the local field is attenuated for induced dipoles along c and enhanced for induced dipoles in the plane. Conversely, L_a is negative for sufficiently small c/a when head-to-tail (eclipsed) dipole interactions dominate. The body-centered lattice has $L = 1/3$ and satisfies the CME at $c/a = 1.134$ and 1.414 in non-cubic environments. At small c/a the strongest interaction in the body-centered lattice is between induced dipoles in eclipsed second-neighbor layers.

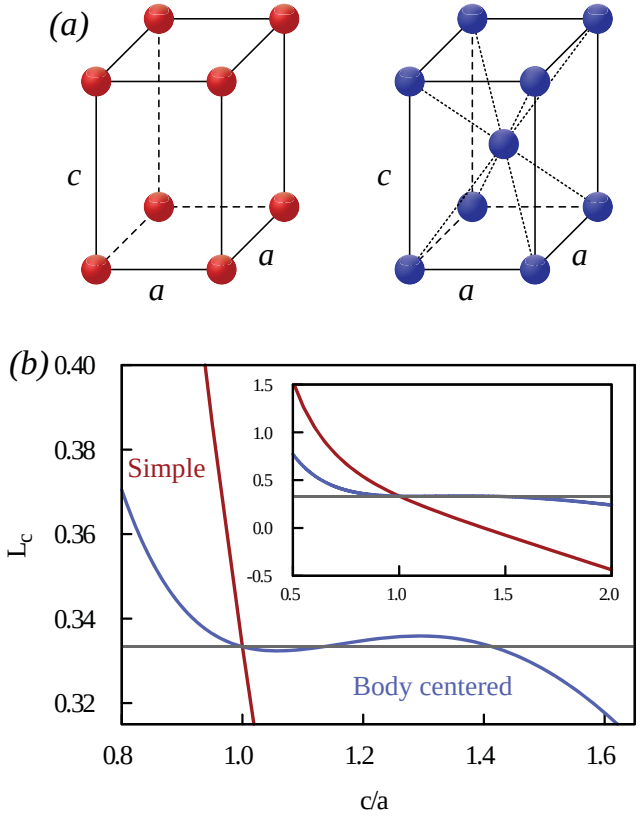

Figure 1. a) Unit cells of simple and body-centered tetragonal lattices; b) Lorentz factor L_c as a function of c/a between 0.80 and 1.65; inset, c/a between 0.5 and 2.0. Tetragonal lattices have $L_a = (1 - L_c)/2$ while cubic ($c/a = 1$) lattices have isotropic $L = 1/3$.

An alternative approach to 3D dipole-field sums is in terms of layers instead of spheres. We define a ML as an infinite plane of polarizable points with Miller indices (hkl). We take the origin at a point in the (001) plane and build a film with thickness $d = (2p + 1)c$ by adding p layers on each side. Uniform polarization is assumed; surface effects are deferred to Section 3. Similarly, the (100) or (010) plane defines a ML and films with $d = (2p + 1)a$. For simplicity, we always apply E normal to the ML (i.e., the film's surface), which is the experimentally relevant direction, and has depolarization $D = 1$. Identical results are obtained with E in the plane and $D = 0$.

Dipole-field sums are evaluated layer by layer. For E and induced dipoles normal to (001), the dipole field at the origin is along c with

$$4\pi\Lambda_{cc}(p) = \sum_{l=-p}^{l=p} K_l(c/a)$$
$$K_l(c/a) = \frac{c}{a}\sum_{n,m}{}' \frac{2(lc/a)^2 - n^2 - m^2}{\left(n^2 + m^2 + (lc/a)^2\right)^{5/2}} \quad (6)$$

The $n = m = 0$ term is excluded in $K_0(c/a)$. The ML sum is depolarizing and equal to $-cK/a$, where $K = 9.033622$ for a square lattice is the Topping constant.[17] Direct summation within a circle of radius ρ about the origin converges absolutely as ρ^{-1}. It was immediately recognized that contributions from layers $l = \pm1, \pm2, \ldots$ decrease exponentially.[18] **Table 1** lists K_l up to $l = 3$ for $c/a = 0.8$, 1.0 and 1.2. Adjacent layers are polarizing, increasing the dipole field; the $n = m = 0$ points are eclipsed. The decrease of $K_1(c/a)$ in **Figure 2** is exponential for $c/a > 1$.

The body-centered tetragonal lattice has two points per unit cell. Since every other layer is staggered, we modify Equation 6 by shifting the in-plane sites for odd values of l and call the new sum $K'_{2l+1}(c/a)$,

$$K'_{2l+1}(c/a) = \frac{c}{2a}\sum_{n,m}{}' \frac{2\left((2l+1)c/2a\right)^2 - (n+1/2)^2 - (m+1/2)^2}{\left((n+1/2)^2 + (m+1/2)^2 + \left((2l+1)c/a\right)^2\right)^{5/2}} \quad (7)$$

Staggered layers are usually depolarizing, which decreases the dipole field. Since we are interested in films with similar

Table 1. Dipole-field sums $K_l(c/a)$, Equation 6, at lattice points in layer 0 due to induced dipoles along c in layer l of simple tetragonal lattices with $c/a = 0.8$, 1.0 and 1.2.

Layer, l	c/a		
	0.8	1.0	1.2
0	−7.226897	−9.033622	−10.840346
1	0.993822	0.327465	0.107134
2	0.005559	0.000555	0.000054
3	0.000036	0.000001	0.000000

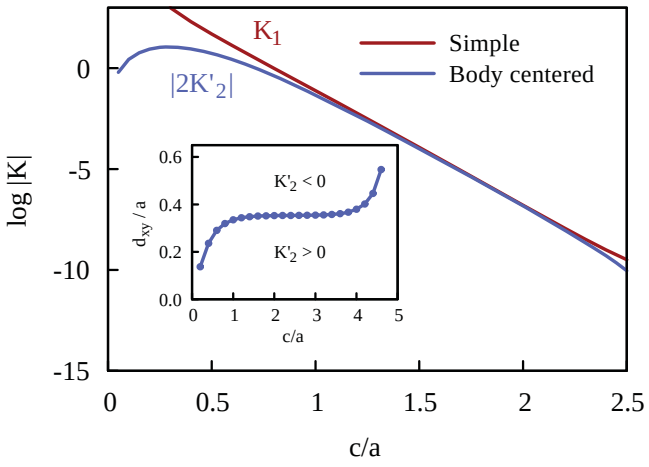

Figure 2. Dipole-field sums K_1, Equation 6, for an infinite eclipsed layer at c/a in a simple tetragonal lattice and $|K'_2|$, Equation 6, for infinite staggered layer at c/a in a body-centered tetragonal lattice. Inset: Offset $x = y = d_{xy}/\sqrt{2}$ of (001) planes at which $K'_2(c/a) = 0$.

spacing in and between planes, the representative values in **Table 2** are for $c/a = 1.5$, 2.0, and 2.5.

The function $|2K'_2(c/a)|$ in Figure 2 has $l = 1/2$ in order to compare the c/a dependence of staggered and eclipsed square-planar layers. We remark that $K'_2(c/a) = 0$ at $c/a = 4.70$ and is polarizing at larger c/a when the induced dipoles are almost eclipsed. Hence $|2K'_2(c/a)|$ is clearly not exponential. But as shown in Tables 1 and 2, the dipole field at the origin decreases so rapidly that limiting contributions to adjacent layers is often an excellent approximation. We can shift adjacent planes such that $K'_2(c/a;d_{xy}) = 0$ when Equation 7 has $(n + x)$, $(m + x)$ with $x = d_{xy}/\sqrt{2}$ instead of $x = 1/2$; the inset of Figure 2 shows the offset $d_{xy}/a \le 1/\sqrt{2}$ at which $K_2' = 0$ as a function of c/a.

We conclude this Section by computing the Lorentz factors $L_c(c/a)$ of tetragonal lattices layer by layer. First, starting with a (001) ML and E along c, we add p layers on either side until $\Lambda_{cc}(c/a)$ in Equation 6 has converged and take $D = 1$ to find L_c; the bulk or crystal limit is reached for $p \sim 5 - 10$. Second, starting with a (100) ML and E along a, we add p layers on either side and take $D = 1$ in Equation 6 to obtain L_a and then $L_c = 1 - 2L_a$. Bulk values of L_c are listed in **Table 3** at $c/a = 0.8$, 1.0 and 1.2. The same results hold with E in the plane and $D = 0$ in Equation 5. As expected, dipole-field sums in 3D depend on the order of summation in Equation 3 and on the orientation of induced dipoles. Nevertheless, identical

Table 2. Dipole-field sums at lattice points in layer 0 due to induced dipoles along c in layer l of body-centered tetragonal lattices with $c/a = 1.5$, 2.0 and 2.5; staggered layers, K' in Equation (7), for odd l, eclipsed layers, K in Equation 6, for even l.

Layer, l	c/a		
	1.5	2.0	2.5
0	−6.775216	−9.033622	−11.292027
1	−0.844712	−0.263449	−0.072401
2	0.009832	0.000555	0.000030
3	−0.000085	−0.000001	0.000000

Table 3. Lorentz factors $L_c(c/a)$ for simple and body-centered tetragonal lattices and $L_z(c/a)$ normal to monolayers in (001), (100), and (010) planes; $L_a = (1 - L_c)/2$.

Lattice		c/a		
		0.8	1.0	1.2
simple	bulk	0.58396	1/3	0.15441
	ML (001)	0.42490	0.28113	0.13735
	(100),(010)	0.17657	0.28113	0.33307
body centered	bulk	0.37046	1/3	0.33479
	ML (001)	0.71245	0.64056	0.56868
	(100),(010)	0.58827	0.64056	0.56654

anisotropic $f = F/E$ are computed in Equation 5 for crystals. Depolarization factors in ellipsoidal samples resolve completely the conditional convergence of 3D dipole-field sums.

Purvis and Taylor[13] generalized the CME to orthorhombic lattices with scalar α and Lorentz factors L_j ($= L_a$, L_a, L_c in tetragonal lattices). After correcting a typo, Equation 34 in a previous study[13] reads

$$\frac{\kappa - 1}{1 + (\kappa - 1)L} = 4\pi n\alpha \tag{8}$$

Scalar α leads in general to tensor κ. The principal components of κ are the Lorentz factors L_j and yield the CME, Equation 2, with $L = 1/3$ for cubic lattices. L_j for MLs in Table 3 illustrate large variations in 2D that always converge to the bulk value in thick films. The (001) ML is the $c >> a$ limit of 3D tetragonal lattices. The (001) Lorentz factors for MLs in Table 3 deviate from 1/3 and decreases with c/a because constant $n = 1/a^2c$ increases depolarizing interactions within the plane. The simple lattice has $L_c < 0$ for $c/a > 1.3988$ and highly anisotropic κ. Equation 8 holds for uniformly polarized samples, a condition that is satisfied in the bulk and by symmetry for a ML, but not for multilayer films. Induced dipoles at or near the surface of multilayer films may deviate from the bulk. Uniform polarization turns out to be a good approximation for some parameters and a poor approximation for others.

3. Tetragonal Thin Films

The requirement of equal local fields F_r is satisfied within every (infinite) layer, but surface and bulk layers have unequal F_r in general. The enhancement f for E normal to the film ($D = 1$) is

$$F_r / E = f_r = 1/\left(1 - 4\pi n\alpha(1 + \Lambda_r)\right) \tag{9}$$

The dipole field $4\pi\Lambda_r$ for a ML is the $l = 0$ term in Equation 6 while Λ for the surface layer also has contributions from neighboring layers on one side and Λ in interior layers has contributions from layers on both sides.

When interlayer dipole fields are retained in Equation 3, scalar α and constant E generates a system of $2p$ linear equations for F_r in $2p$-layer films. Direct solution now requires an explicit choice of αn. Clearly, f_r is small when αn is small and the layer

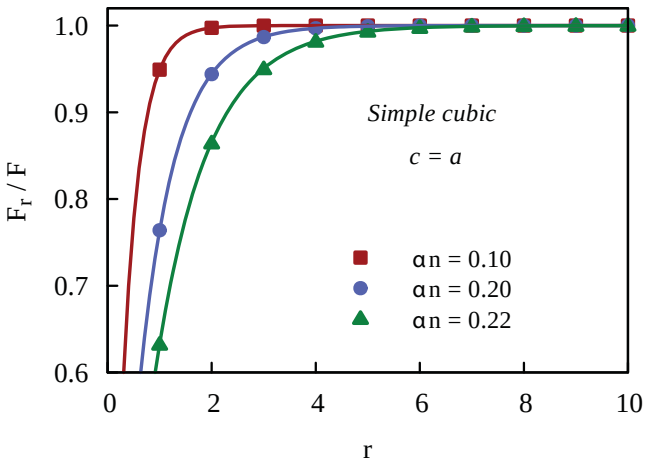

Figure 3. Ratio F_r/F of local fields in the surface layer, $r = 1$, and interior layers, $r > 1$, to F at the center. The simple cubic film has 100 layers with (001) surfaces and applied field normal to the surface. Points are direct solution of Equation 9; lines are the analytical model, Equation 10, with continuous r.

dependence of $(1 + \Lambda)$ is just a small correction. But interlayer interactions become strong for $c < a$ and increasing αn always increases f_r. All reported numerical results are solutions of Equation 3 for (001) films of 100 layers with induced dipoles normal to the films and identical surfaces at $r = 1$ and $r = 100$.

We compute F_r/F, the ratio of the local field at layer r to the local field at the center of the film. **Figure 3** shows the dependence of F_r/F on αn in a simple cubic lattice calculated using the values of $K_0(1)$ and $K_l(1)$ in Table 1. Since K_1 is polarizing, we expect and find $F_1/F < 1$ at the surface. Increasing αn strongly enhances surface effects, again as expected in view of divergent f in the bulk at $\alpha n = 3/(4\pi)$. Moreover, since interlayer interactions increase for $c < a$, surface effects also depend on structure.

To model the surface effects analytically, we limit interlayer interactions to adjacent layers while almost retaining the bulk value of F. More precisely, we take $K_{eff}(c/a) = K_1 + K_2$ and treat the surface of a semi-infinite film with a (001) face. The local field in layers $r = 2, 3,...$ is given by

$$F_r(1-\alpha n[4\pi + K_0(c/a)]) = E + \alpha n K_{\text{eff}}(c/a)[F_{r+1} + F_{r-1}] \qquad (10)$$

Given that the surface layer $r = 1$ presents only F_2 in Equation 10, the solution is

$$F_r/F = 1 - \exp(-r\Gamma)$$
$$\cosh\Gamma = \frac{1-\alpha n[4\pi + K_0(c/a)]}{2\alpha n K_{\text{eff}}(c/a)} \qquad (11)$$

Lines in Figure 3 are obtained from Equation 11 with continuous r and show the exponential increase from surface to bulk. The excellent analytical fits quantify the dependence of surface effects on αn and structure. The generalized CME is a good approximation for $\Gamma > 3$ when the surface layer already has $F_1/F > 95\%$. Although limited to neighbors, strong interlayer interactions extend surface effects deep into the film. The condition $\cosh\Gamma \geq 1$ ensures a positive denominator in Equation 9.

Surface effects in body-centered tetragonal lattices are qualitatively different as shown in **Figure 4** for (001) films with $c = 2a$ and variable αn. F_1/F is enhanced relative to the interior when neighboring layers are depolarizing. Increasing αn or interlayer interactions again increases surface effects. The analytical model with K_{eff} is still described by Equation 10 but the solution in Equation 11 differs for $K_{eff} < 0$ as follows: we have $F_r/F = 1 - (-1)^r\exp(-r\Gamma)$ and $|K_{eff}|$ in the denominator. The analytical results are quantitative for these parameters; deviations from the calculated values are within the symbols in Figure 4. We note that $\cosh\Gamma = 1$ is now satisfied when the denominator of Equation 9 is still positive; in this regime, beyond the scope of this paper, F_r/F fluctuates over all layers.

Tetragonal films are simple enough for approximate analytical treatment and realistic enough to differentiate between eclipsed and staggered layers. Displaced adjacent layers can be used to mimic organic films with tilted molecules relative to the surface or SAMs with tilted oligomers. Surface contributions depend primarily on αn. They increase with αn, as expected since $\cosh\Gamma$ in Equation 11 has decreasing numerator and increasing denominator. Contributions from distant layers decrease rapidly, as shown in Tables 1, 2 and Figure 2. Simple tetragonal lattices present polarizing $K_1(c/a)$ in Equation 6 as we anticipate for eclipsed layers in general. Body-centered tetragonal lattices usually have depolarizing neighbors. Surface effects are minimized if not entirely suppressed along the line $K'_2(c/a,d) = 0$ in the inset to Figure 2.

4. Organic Molecular Crystals

In this Section, we generalize the calculation of relative permittivity in atomic lattices to organic molecular crystals. Unit cells of typical compounds used in organic electronics contain several molecules with anisotropic α and up to $M \sim 10^2$ atoms. In terms of polarizable points, the electric field F_{0s} in Equation 3 has to be evaluated at M atoms, $s = 1, 2, ..., M$, in a uniformly polarized crystal; unit cells are of course equivalent but the

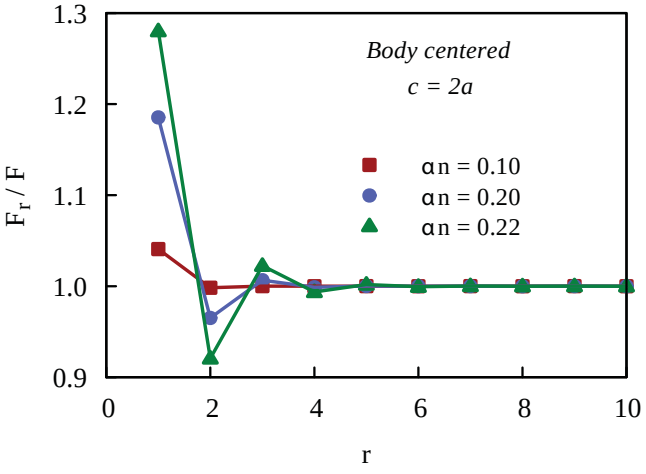

Figure 4. Ratio F_r/F of local fields in the surface layer, $r = 1$, and interior layers, $r > 1$, to F at the center. The body-centered tetragonal film has 100 layers with (001) surfaces and applied field normal to the surface. Points are direct solution of Equation 9; lines are to guide the eye.

F_{0s} at atoms are not. The partitioning of α among polarizable points is left open in ME but never exceeds M. The CR approach[3] includes the electrostatic potential ϕ_s in addition to the field $\boldsymbol{F}_s$ at each atom. Dipole-field sums $\Sigma_m T_{0m}$ are computed at all atoms and unit cells with many atoms are still manageable numerically. Atomic lattices with identical anisotropic α can be treated analytically but are not representative. The principal axes of α and κ coincide in the generalized CME, Equation 8, for cubic crystals with $L = 1/3$, but do not coincide in non-cubic crystals.

The conditional convergence of 3D dipole-field sums is addressed the same way as for the atomic lattices. We choose an origin in a reference unit cell, for example at an atom, define the distance R_p to the same point in the p-th cell, and introduce a variable cut-off R. We apply a uniform static field E along the three orthogonal directions (x,y,z), retain cells with $R_p < R$, find induced dipoles at atoms and compute the elements of the symmetric tensor ζ that relates E to the unit-cell polarization as $\mathrm{P} = \zeta\mathbf{E}$. Increasing R and extrapolation to infinite R leads to

$$\vec{P} \equiv \chi \cdot \vec{F} = \zeta \cdot \vec{E} \tag{12}$$

where $\chi = \kappa - 1$ is the electric susceptibility[9,10] and the Cartesian components ζ_{ij} are obtained directly. Since a uniformly polarized sphere has $F = E - 4\pi P/3$, we solve Equation 12 to obtain[3]

$$\chi = \kappa - 1 = 4\pi\zeta/(1 - 4\pi\zeta/3) \tag{13}$$

The principal axes of κ and ζ are the same, while the principal components are clearly different. The form of Equation 13 is that of a generalized CME.

In the layer-by-layer approach, we apply a uniform field E along x, y and z to a ML in the xy plane, compute $\boldsymbol{F}_s(\rho)$ at each atom due to cells within a circle of radius ρ, and extrapolate to infinite ρ. As in the case of atomic lattices, we add layers above and below the ML, compute their contribution to $\boldsymbol{F}_s$ within the same circle and extrapolate. A few layers, about five, lead to convergent $\boldsymbol{F}_s$. The polarization P is again given by Equation 12, but with a different tensor ζ' for layer-by-layer evaluation of dipole fields. A uniformly polarized film has $F_z = E_z - 4\pi P$ normal to the plane and no depolarization in the plane. Equation 13 now has ζ' instead of ζ and depolarization $4\pi\zeta'$ limited to z components normal to the film. Identical $\chi = \kappa - 1$ are found[19] within numerical accuracy for anthracene crystals and thick films with ab surfaces.

The static dielectric tensor κ of anthracene single crystals has been obtained by different methods and multiple measurements. Charge redistributions (CR) accounts[3] well for κ. D'Avino et al.[20] have recently compared CR and ME results for the dielectric tensors and polarization energies of more than a dozen crystals of molecules used in organic electronics. Both methods are broadly satisfactory.

5. Organic Molecular Films

Molecular films for organic electronics applications typically consist of conjugated molecules. Pentacene films shown schematically in **Figure 5**a have been particularly well characterized. Multilayer films present standing molecules with the largest component of the polarizability, that is, α_{LL} along the

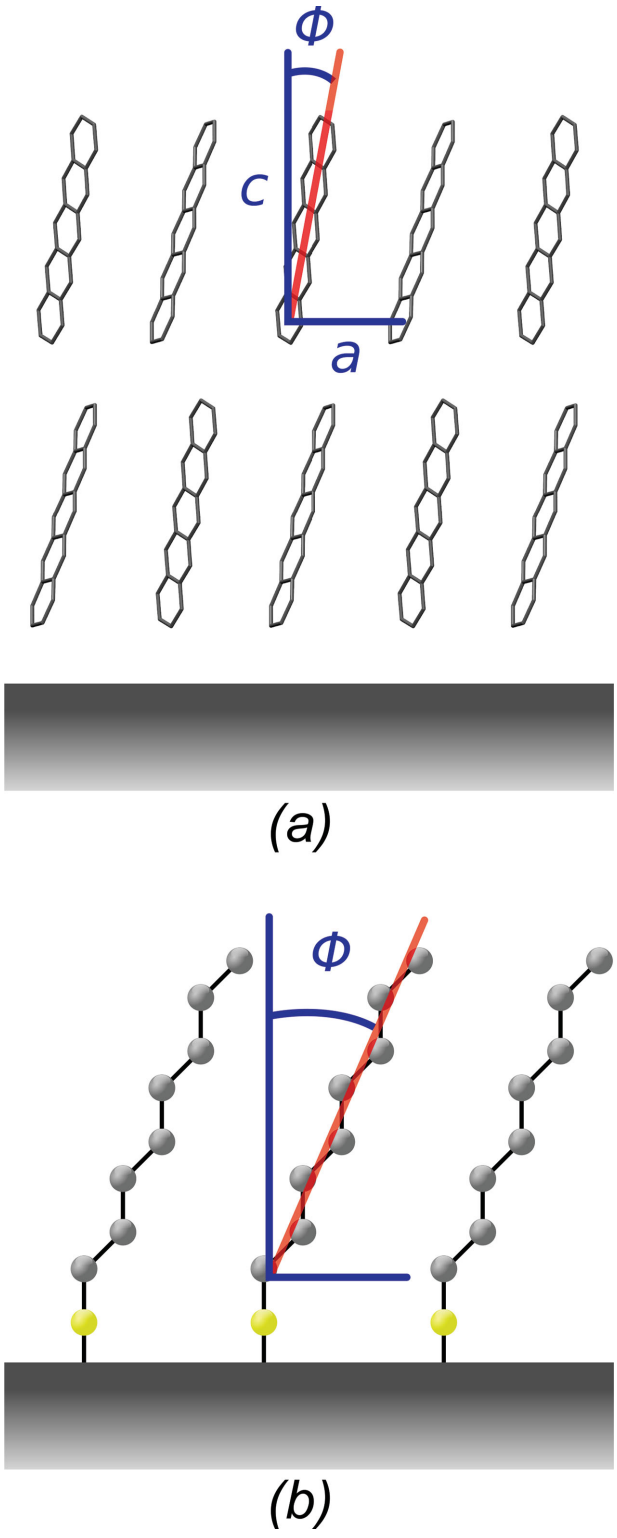

Figure 5. Schematic representations of a) a multilayer pentacene film and b) a self-assembled monolayer (SAM); the angle Φ from the surface normal is the tilt of molecular long axes or of oligomers.

long axis, tilted about $\Phi \approx 30°$ from normal to the crystallographic *ab* plane. Although different in detail and dependent on substrates, the structures of organic molecular films and crystals are broadly similar. The schematic SAM in Figure 5b has nonconjugated oligomers tilted by Φ from the surface normal. We draw attention to Φ, whose role has not been appreciated. In general, Φ reduces the dipole fields of adjacent layers as discussed in Section 2 for simple and body-centered tetragonal lattices.

There are multiple ways of approximating molecular films or SAMs by polarizable points. Polarizable points are associated with monomers such as CH_2 groups in alkylthiolate SAMs whose thickness increases linearly with the number of monomers. ME partitions[1,2] anisotropic α of conjugated molecules. We focus here on the dielectric properties computed for a ME or CR scheme rather than on the specific method. The structure is given and fixes all dipole-field sums that in films are naturally evaluated layer by layer. As noted above for uniformly polarized crystals, layers or spheres return the same tensor κ in Equation 13 when depolarization is taken into account. Since unit cells in a ML are uniformly polarized, the layer method described above for crystals immediately yields κ_{ML}. An important result of the present study is the extension of dielectric calculations to freestanding organic MLs or thin films, and applications to representative films used in organic electronics are in preparation.[21] As in the case of tetragonal atomic films in Section 3, surface effects in multilayer films increase with αn.

To illustrate surface effects in molecular films, we consider a toy model loosely based on the herringbone motif of pentacene or anthracene crystals and films with *ab* faces. The monoclinic anthracene lattice has two molecules per unit cell. The molecular volume is 240 Å^3; the footprint is a^2 = 25.8 Å^2 per molecule in the *ab* plane; the interlayer separation is c = 9.21 Å (c^* in the crystal). As in Figure 5a, the long molecular axis with the largest $\alpha_{LL} \approx 40$ Å^3 is tilted at $\Phi = 34°$ leading to $\alpha_{LL}n \approx 0.17$ for induced dipoles normal to the film and to potentially significant surface contributions similar to those shown in Figure 3. For comparison, the molecular volume of pentacene is about 350 Å^3; delocalization increases α_{LL} to 95 Å^3 and $\alpha_{LL}n$ to 0.27. The footprint in the *ab* plane and van der Waals separations between *ab* layers are almost the same. The toy model for anthracene is a simple tetragonal film with c/a = 1.81, a = 5.08 Å, variable tilt Φ and three points with scalar $\alpha/3$ at the center of rings; pentacene has larger c/a and five points with $\alpha/5$. The extreme approximation of one polarizable point per molecule fails badly since, as shown in Section 2, adjacent layers are depolarizing rather than polarizing at $c/a > 1.4$.

A field normal to (001) generates local fields F_{rs} at the center of ring s of anthracene layer r. The polarization of any cell in layer r is

$$P_r = \frac{\alpha n}{3}(F_{r1} + F_{r2} + F_{r3}) \tag{14}$$

The generalization of atomic films in Equation 9 to the toy model for anthracene films reads

$$\begin{aligned} F_{rs}(1-\alpha n C_{rs}) &= E + \alpha n \sum_{s' \neq s} C_{rs'} + \alpha n \sum_{r' \neq r, s'} C_{r's'} \\ C_{rs} &= (4\pi + K_0^0)/3 \\ C_{rs'} &= (4\pi + K_0^{s'})/3 \qquad s' \neq s \\ C_{r's'} &= K_{rs}^{rs'}/3 \qquad r' \neq r \end{aligned} \tag{15}$$

The dipole-field sums K_0^s correspond to Equation 6: $K_0{}^0$ is due to the same rings as s while $K_0^{s'}$ is due to other rings in the same layer and $K_{rs}^{r's'}$ to rings s' in layers other than r.

We solved films of 20 layers for different αn and Φ. **Figure 6** shows F_{rs}/F at one surface for upright molecules with $\Phi = 0$ and tilted molecules with $\Phi = 35°$. The bulk values are independent of r, as required, but the local fields are not equal at the central ring s = 2 and outer rings s = 1, 3. Surface effects increase with αn and decrease with Φ. Although adjacent layers account quantitatively for dipole fields, upright molecules already have stronger surface effects at αn = 0.05 than tilted molecules at αn = 0.10. The toy model confirms the importance of molecular tilt. Polarizable points in actual structures can then readily be modeled layer by layer. CR calculation[19] of anisotropic κ of an anthracene ML with *ab* surfaces is within a few percent of the bulk value.

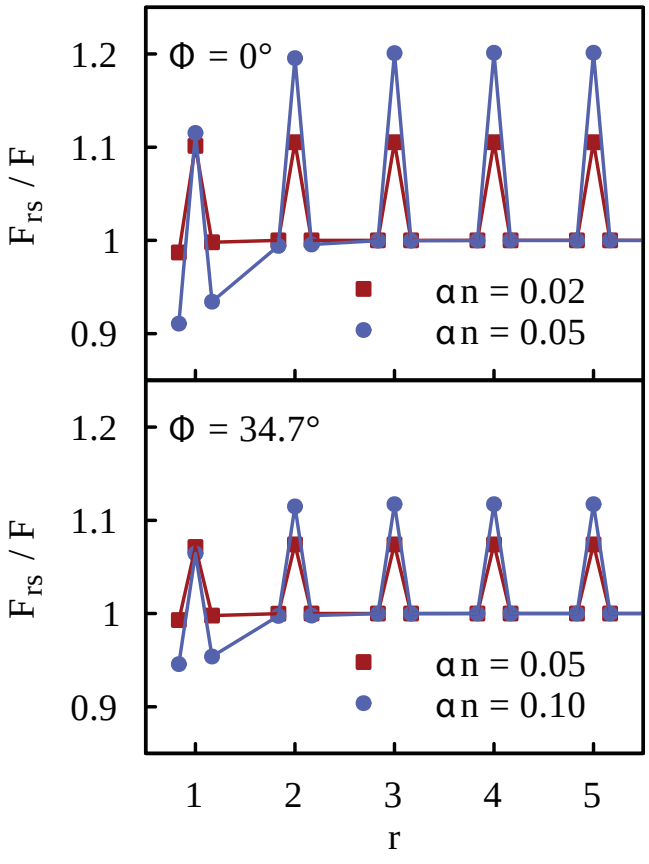

Figure 6. Ratio F_{rs}/F of local fields in the surface layer, r = 1, and interior layers, $r > 1$, to F at points s = 1 or 3 at the center. The film has 20 layers r with three points s per unit cell. Points are direct solution of Equation15; lines are to guide the eye.

Next we turn to films discussed by Natan et al.[8] in a detailed theoretical and DFT study that illustrates nicely how to model dielectric properties using polarizable points. Oligophenyls, H-$(C_6H_4)_N$-H with N = 1 – 10, are linear molecules with σ bonds at para positions and weak electronic coupling between phenyl rings. When E is applied along the oligomer, the polarizability α_N can be computed directly and, as shown in Figure 1a in a previous study,[8] α_N increases much faster than $N\alpha$, where α = 12.45 Å^3 is the monomer value. A polarizable point α at the center of each ring leads to interactions between induced dipoles that account well for α_N. Natan et al.[8] analyzed DFT calculations on a ML of oligomers that form an orthorhombic lattice with a' = 3.83, b' = 6.64 Å and eclipsed (Φ = 0) layers with c = 4.3 Å per oligomer; they also studied a "sparse" monolayer with 2a' and 2b'. In effect, they varied oligomer length and density at constant α and c. We take instead a simple tetragonal lattice with a = 5.04 Å, c/a = 0.85, the same unit-cell volume and αn = 0.114 for a ML; the sparse ML has $c/2a$ = 0.43 and αn = 0.075.

The polarizability profile α_i/α_{max} shown in Figure 2b of the same previous study[8] for decaphenyl films is closely related to F_r/F in Figure 3 for 100-layer films. The induced dipole in layer i is $\mu_i = \alpha F_i/F_{ext}$ and α_i/α_{max} is normalized with respect to the interior of the film. The calculation was carried out without depolarization: F_{ext} is applied normal to the film and Equation 5 is solved with the dipole-field sum Λ but without D. Consequently, interactions between oligomers reduce α_i. Later on, Natan et al.[8] emphasized that depolarization leads to enhanced α_i and eventually to the CME in thick cubic films. We relax the restriction to cubic lattices and, as shown for tetragonal lattices, can follow the evolution of dielectric properties from ML to multilayer to bulk with the aid of Lorentz factors.

The in-plane contribution $\alpha n K_0$ to the dipole field in Equation 6 is $-\alpha K/a^3$. The contribution $\alpha n K_1$ of an eclipsed adjacent layer is $2\alpha/c^3$ in the limit $a >> c$ when the $n = m = 0$ term dominates in Equation 6 and interactions between induced dipoles within an oligomer are the largest. To discuss Figure 2b of Natan et al.,[8] we solve Equation 9 without the depolarization factor D. The analytical approximation in Equation 11 now reads

$$F_r/F = 1 - \exp(-r\Omega)$$
$$\cosh\Omega = \frac{1+\alpha K/a^3}{2\alpha n K_{eff}(c/a)} \geq \frac{2c^3}{9\alpha} \quad (16)$$

Here $K_{eff} = K_1 + K_2$ and the $a >> c$ limit of isolated oligomers is a lower bound on Ω since the numerator increases while the denominator decreases with increasing c/a. The bound returns Ω = 0.89 and F_1/F = 0.59, in agreement with α_1/α_{max} = 0.60 for oligomers.[8] The ML with a = 5.04 Å, c/a = 0.85 and $n = 1/a^2c$ has $2\alpha n K_{eff}$ = 0.172, Ω = 3.08 and F_1/F = 0.95, again matching[8] α_1/α_{max} = 0.95 and reduced surface effects in the ML. The sparse ML with c/a = 0.43 has $2\alpha n K_{eff}$ = 0.485, Ω = 1.47 and F_1/F = 0.77, while[8] α_1/α_{max} = 0.77. The field F or $\alpha_{max} = \mu/F$ in the interior of a film without depolarization is given by

$$\alpha_{max} = \frac{\alpha}{1+\alpha K a^{-3} - 2\alpha n K_{eff}} \quad (17)$$

The upper bound is the oligomer limit, α_{max} = 42 Å^3, just as reported,[8] as is α_{max} = 20 and 7.3 Å^3 for the sparse and standard ML, respectively. Equation 17 illustrates the balance between depolarizing interactions within layers and polarizing interactions between layers. The analytical model reproduces the direct computations on oligophenyl films.

6. Discussion

The CME, Equation 2, relates the product of the polarizability and number density, αn, to the relative permittivity $\kappa = \varepsilon/\varepsilon_0$ of a gas or dilute liquid of neutral atoms or molecules whose positions are random. The average (trace) α for molecules accounts for random orientation. The CME is retained for isotropic (scalar) α in uniformly polarized cubic lattices with Lorentz factors L = 1/3. We showed that the generalized CME also holds for uniformly polarized atomic lattices of lower symmetry with anisotropic Lorentz factors that lead to tensor κ as indicated in Equation 8. The key variable is $\alpha n L_j$ for induced dipoles along the j-th principal axis. The conditional convergence of 3D dipole-field sums is resolved by Lorentz factors in ellipsoidal samples that support uniform polarization, including thin films. As emphasized in Table 3 for tetragonal lattices, identical L_c and L_a are computed in spherical crystals or in thick films with (001), (100) or (010) faces. We have verified that the layer-by-layer approach to dipole-field sums discussed in Section 4 returns the same anisotropic κ of anthracene crystals as computed using spheres.

The layer by infinite layer approach is well suited for the dielectric properties of (idealized) thin films. A uniform field normal to a classical surface induces a continuous uniform dipole density. A dipole density generates[9] a potential jump across the surface that corresponds exactly to a depolarization factor D = 1. Since the potential is constant, the dipole field vanishes on either side of the plane. Hence fields generated by discrete induced dipoles normal to the surface vanish within a few lattice constants. It follows that dipole fields between infinite layers are extremely short-ranged[6,8,18] and can be treated analytically when limited to adjacent layers. DFT calculations with E normal to the surface yield κ_{zz}, which in general is not a principal component. The full tensor κ can be estimated for molecular films in the limit of no intermolecular overlap, and such calculations[21] are in progress for representative molecular films with organic electronics applications.

However, short-range dipole fields do not guarantee small surface contributions in general. Polarization near the surface deviates from the bulk and deviations increase with αn as shown in Figure 3,4 6. The generalized CME holds up to about 10% deviation between surface and bulk. Given the structure and αn, surface contributions can be estimated using Equation 11 for eclipsed atomic layers or its modified version for staggered layers. The generalization to molecular films of polarizable points in Equation 15 is straightforward but has not been explored so far.

Microlectrostatic (ME) representations of molecules as polarizable points or charge redistribution (CR) within conjugated molecules provide a unified approach to the dielectric properties of organic films of closed-shell molecules with small intermolecular overlap. The molecular polarizability accounts reasonably well for long-range electrostatic interactions and relates organic molecular films and SAMs to the wider literature on dipoles, induced dipoles and electrostatic interactions. It must be kept in mind, however, that the approximation of no intermolecular overlap precludes charge-transfer states and can be relaxed in quantum calculations of small molecular clusters.

Acknowledgements

Z.G.S. thanks G. D'Avino for stimulating correspondence about the dielectric properties of films. The authors thank the National Science Foundation for partial support of this work through the Princeton MRSEC (DMR-0819860).

Received: July 18, 2014
Revised: September 16, 2014
Published online: October 22, 2014

[1] E. A. Silinsh, V. Cápek, *Organic Molecular Crystals: Interaction, Localization, and Transport Phenomena*, AIP Press, New York **1994**, and references therein.
[2] J. W. Rohleder, R. W. Munn, *Magnetism and Optics of Molecular Crystals*, Wiley, New York **1992**, and references therein.
[3] E. V. Tsiper, Z. G. Soos, *Phys. Rev. B* **2001**, *64*, 195124.
[4] R. Clausius, *Die Mechanische Warmetheorie II*, Vieweg, Braunschweig **1879**, p 162.
[5] O. F. Mossotti, in *Rendiconti dell'Accademia Nationale della Scienze detta dei XL. Vol. XXIV, No. 40*, **1850**, p. 49.
[6] P. B. Allen, *J. Chem. Phys.* **2004**, *120*, 2951.
[7] G. D. Mahan, *Phys. Rev. B* **2006**, *74*, 033407.
[8] A. Natan, N. Kuritz, L. Kronik, *Adv. Funct. Mater.* **2010**, *20*, 2077.
[9] J. D. Jackson, *Classical Electrodynamics*, Wiley, New York **1962** p 119.
[10] C. Kittel, *Introduction to Solid State Physics*, 5th Ed, Wiley, New York **1976**, p 410.
[11] H. Mueller, *Phys. Rev.* **1935**, *47*, 947.
[12] J. H. P. Colpa, *Physica* **1971**, *56*, 185, 205.
[13] C. K. Purvis, P. L. Taylor, *Phys. Rev. B* **1982**, *26*, 4547.
[14] a)B. R. E. Nijboer, F. E. De, *Wette, Physica* **1957**, *24*, 422; b) S. W. de Leeuw, J. W. Perram, E. R. Smith, *Proc. R. Soc. Lond. A* **1980**, *373*, 27; c) H. Leon, E. Estevez-Rams, *J. Phys. D: Appl. Phys.* **2009**, *42*, 185012.
[15] a) F. G. Amar, J. Smaby, T. J. Preston, *J. Chem. Phys.* **2005**, *122*, 244717; b) M. Tchaplyguine, R. R. Marinho, M. Gisselbrecht, J. Schulz, N. Mårtensson, S. L. Sorensen, A. Naves de Brito, R. Feifel, G. Öhrwall, M. Lundwall, S. Svensson, O. Björneholm, *J. Chem. Phys.* **2004**, *120*, 345.
[16] a) J. A. Osborn, *Phys. Rev.* **1945**, *67*, 351; b) E. C. Stoner, *Philos. Mag.* **1945**, *36*, 803.
[17] J. Topping, *Proc. R. Soc. London, Ser. A* **1927**, *114*, 67.
[18] J. E. Lennard-Jones, M. Dent, *Trans. Faraday Soc.* **1928**, *24*, 92.
[19] G. D'Avino, Z. G. Soos, unpublished.
[20] G. D'Avino, L. Muccioli, C. Zannoni, D. Beljonne, Z. G. Soos, *J. Chem. Theory Comput.*, **2014**, DOI: 10.1021/ct500618w.
[21] D. Vanzo, G. D'Avino, Z. G. Soos, unpublished.